Supplementary material to: Bayesian parameter estimation and interpretation for an intermediate model of tree-ring width

S.E. Tolwinski-Ward, K.J. Anchukaitis, M.N. Evans

In the following we present supplementary information as referenced in the text of the associated research article, 'Bayesian parameter estimation and interpretation for an intermediate model of tree-ring width'.

Form of error model for white and AR(1) noise models For the white noise model: $\Sigma_e = \sigma_W^2 I$. For the AR(1) model, we use the approximation: $\Sigma_e \approx (I - \phi_1 B)^{-1}(\tau^2 I)\Big((I - \phi_1 B)^T\Big)^{-1}$ where B is the matrix representation of the backshift operator (ones on the first subdiagonal and zeros everywhere else). This follows from the AR(1) specification of the error model, which can be written $e_t - \phi e_{t-1} \sim N(0, \tau^2)$, or in matrix form, as $(I - \phi_1 B)\boldsymbol{e} \sim N(0, \tau^2 I)$.

Representative trace plots of MCMC chains To give readers a sense of the MCMC output, here we show trace plots of three MCMC chains before subsampling for the PPE with SNR = 1 at Sipsey Wilderness site, for which priors and posteriors are shown in Figure 1 of the manuscript:

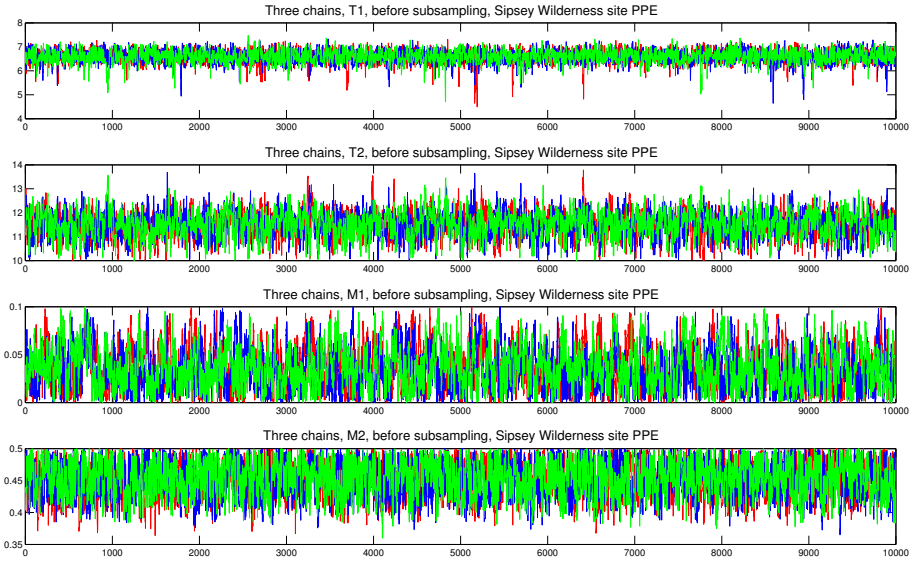

Figure 1: Trace plots of three MCMC chains sampling the VS-Lite growth-response parameters conditioned pseudoproxy data and PRISM data co-located with the Sipsey Wilderness site. Chains are shown before sub-sampling meant to reduce autocorrelation in the samples.

Details of reproducibility experiments Here we provide tables of statistics computed from two independent posterior draws which were sampled as described in the text for two representative sites, for the setting of the PPE with SNR = 1 and the OPMC setting.

	Sipsey Wilderness Site, AL		Mammoth Creek Site, UT	
PPE Statistic	Draw 1	Draw 2	Draw 1	Draw 2
median T_1	6.0591 °C	5.9704°C	5.1315 °C	5.1552 °C
median T_2	16.0761°C	16.0894°C	13.1334 °C	13.0954 °C
median M_1	0.0368 v/v	0.0373 v/v	0.0485 v/v	0.0480 v/v
median M_2	0.4081 v/v	0.4077 v/v	0.4125 v/v	0.4115 v/v
post/prior variance, T_1	0.6891	0.7371	0.1978	0.1925
post/prior variance, T_2	0.2747	0.2817	0.1407	0.1391
post/prior variance, M_1	1.0461	1.0491	0..9094	1.0113
post/prior variance, M_2	0.0432	0.0432	0.1389	0.1444
$\hat{\text{SNR}}$	0.5173	0.5164	0.7260	0.7259

Table 1: Posterior statistics to four decimal places, computed from two separate MCMC draws conditioned on pseudoproxy data with SNR = 1 at the Sipsey Wilderness site in Alabama, where the white noise model is used, and at the Mammoth Creek site in Utah, where the AR(1) error model is employed. Estimates are for one realization of pseudoproxy data and noise.

	Sipsey Wilderness Site, AL		Mammoth Creek site, UT	
OPMC Statistic	Draw 1	Draw 2	Draw 1	Draw 2
median T_1	4.8599°C	4.8956°C	6.4310°C	6.4412°C
median T_2	12.9649°C	13.0301°C	16.2687°C	16.2361°C
median M_1	0.0567 v/v	0.0559 v/v	0.0392	0.0370
median M_2	0.3971 v/v	0.4006 v/v	0.4204	0.4217
post/prior variance, T_1	1.1052	1.0724	1.0148	1.0348
post/prior variance, T_2	0.3157	0.3527	0.4393	0.4660
post/prior variance, M_1	1.0176	1.0482	1.0857	1.0868
post/prior variance, M_2	0.1938	0.1904	0.4891	0.4578
$\hat{\text{SNR}}$	0.6612	0.6588	0.4531	0.4637

Table 2: As in Table 1, but for observed data.

Posterior to prior variance ratios for PPE with SNR = 0.25 We provide here a map of the ratio of prior to posterior variance for the PPE with lower signal-to-noise ratio for comparison to the one shown in the research article for SNR = 1.

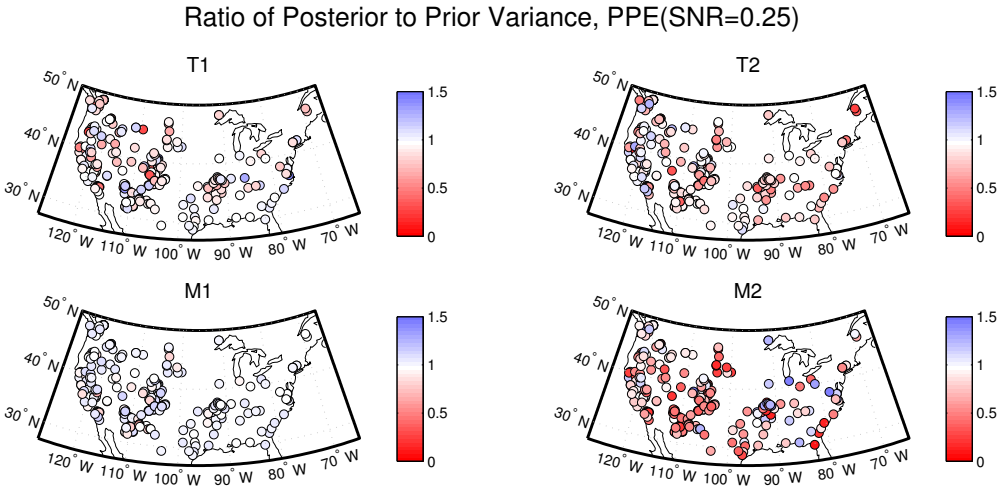

Figure 2: Ratio of posterior to prior variance for the four growth response parameters as a measure of Bayesian learning in the pseudoproxy experiment with SNR = 0.25. Color scale calibrated so that sites with smaller (larger) values of the ratio, indicating greater (lesser) Bayesian learning, have darker (lighter) coloration.

Sensitivity analysis using uniform priors Here we present parameter estimation results for the observed data model calibration using uniform priors.

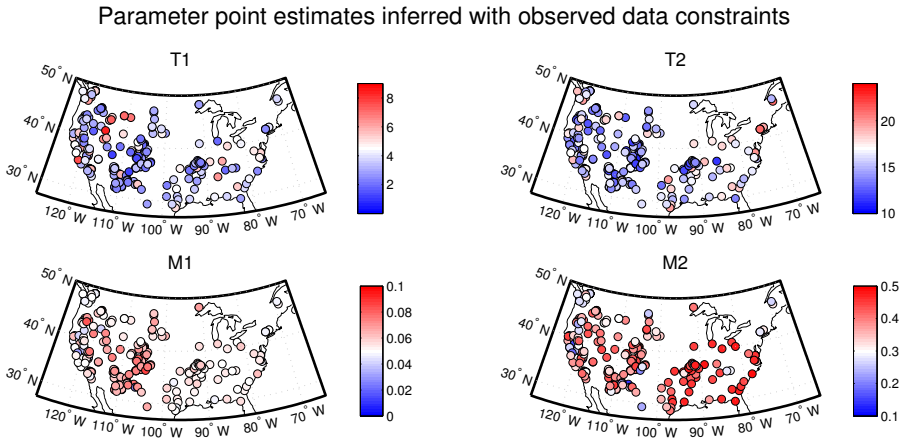

Figure 3: As in Figure 4 in the associated article, but for parameters estimated using uniform priors.

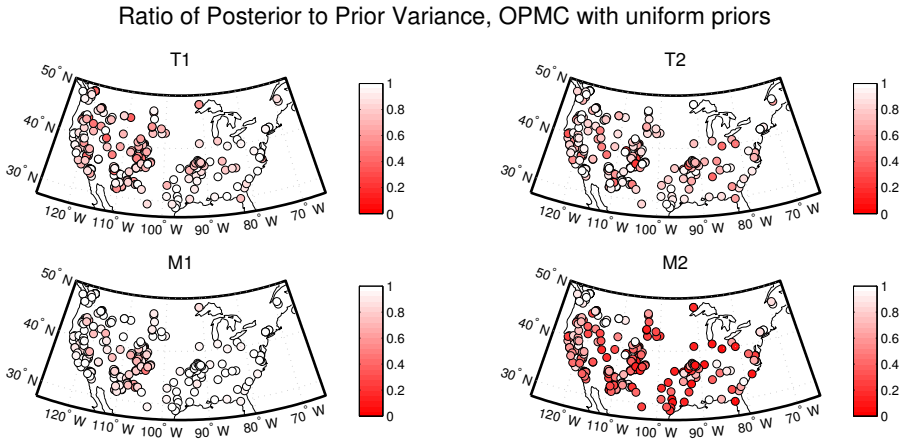

Figure 4: As in Figure 5 in the associated article, but for posteriors estimated using uniform priors.

Medians of marginal parameter posteriors as summary statistics Although the medians of the marginal posteriors are not in general global medians, here we present pairwise scatterplots of the distribution of parameter draws with the pairs of marginal medians plotted on top at a representative site. The form of our posteriors are simple enough so that the vector of marginal parameter medians provides a reasonable representation of the center of the distribution.

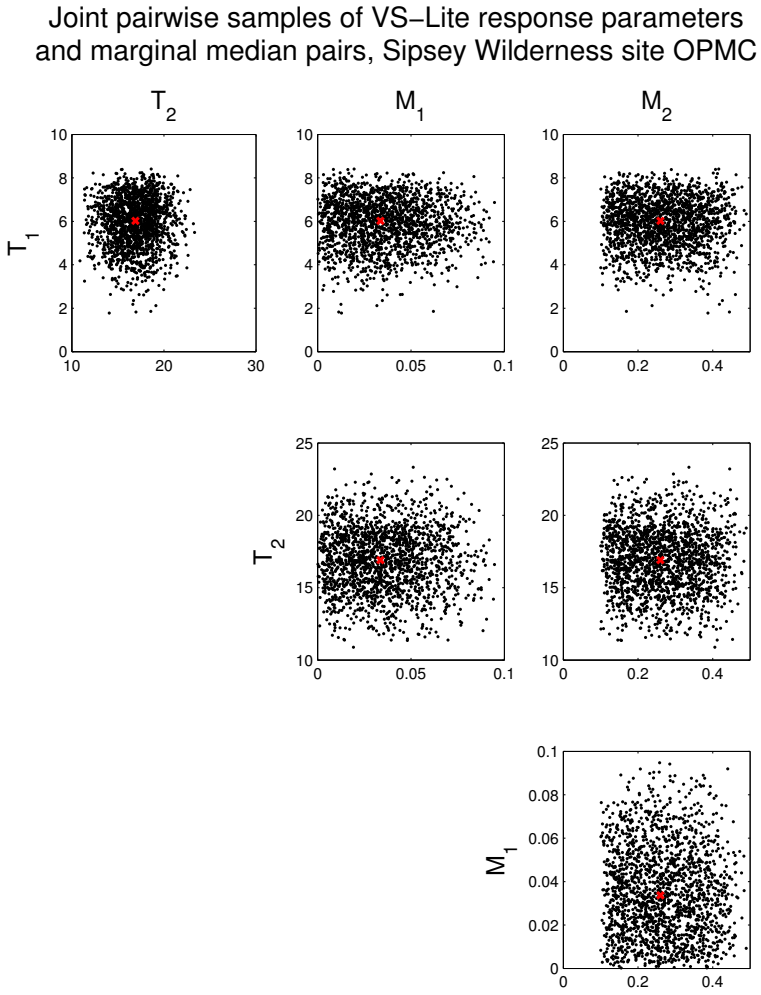

Figure 5: Pair-wise scatter plots of growth response parameter samples, with marginal posterior median values plotted on top in red.

Sensitivity experiment results The point estimates of the parameters derived from scientifically-based priors and uniform priors are most similar for sites with high posterior-to-prior variance ratios, and tend to fall much closer to the boundaries of their prior support when uniform priors are used.

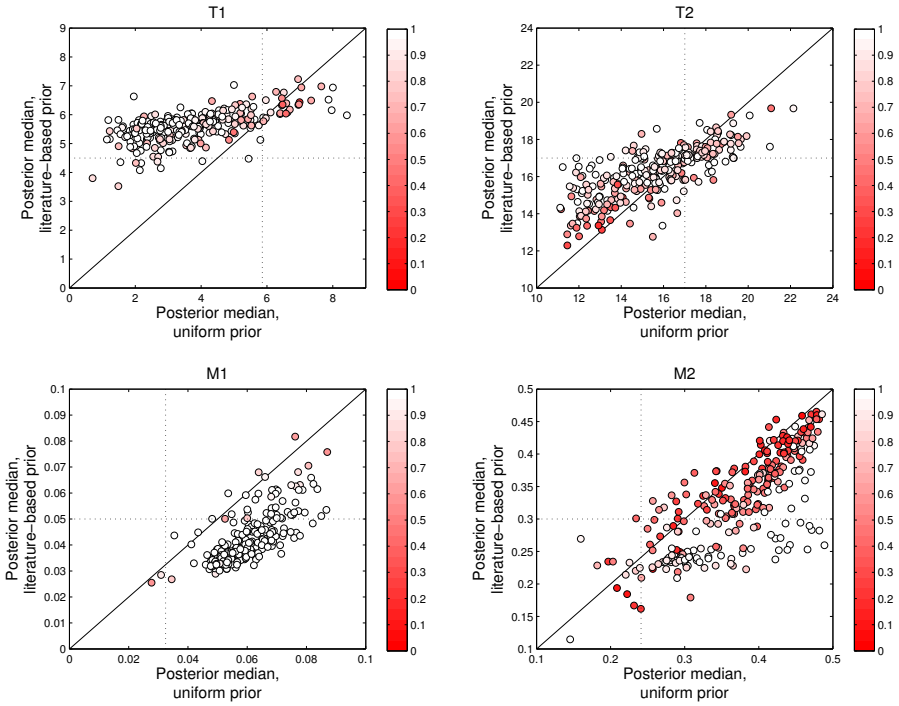

Figure 6: Posterior medians at 277 sites for the four growth response parameters estimated from scientifically-informed priors versus uniform priors for the OPMC. The color of the points gives the ratio of posterior to prior variance in the model calibration run using literature-based priors.

Spatial structure of calibrated model residuals Our approach treats VS-Lite residuals at distinct sites as conditionally independent given the underlying spatially-covarying climate. However, the model residuals may in practice covary across space given the limitations of VS-Lite. To investigate the spatial structure of the model residuals, we compute the maximum likelihood fit of a spatial model assuming exponential covariance structure to the residuals of simulations performed with parameters everywhere held at the posterior medians, and to simulations using the site-by-site calibrated parameters. The ratio of "spatial signal-to-noise" is reduced in the latter case, with the ratio of spatial process variance to nugget variance (interpretable as measurement error) being 1.58 for the field of uncalibrated residuals, and 1.08 for the field of calibrated residuals. The range parameter of the spatial covariance is also reduced for the calibrated residual field (1.56 compared to 1.92, in degrees of lat/lon), indicating that the remaining spatial structure is more localized after calibration. Here we also show a spatial plot of RMSE across all sites and simulation years, which appears uniform to first order across space, although there are some regional deviations from the domain-wide mean.

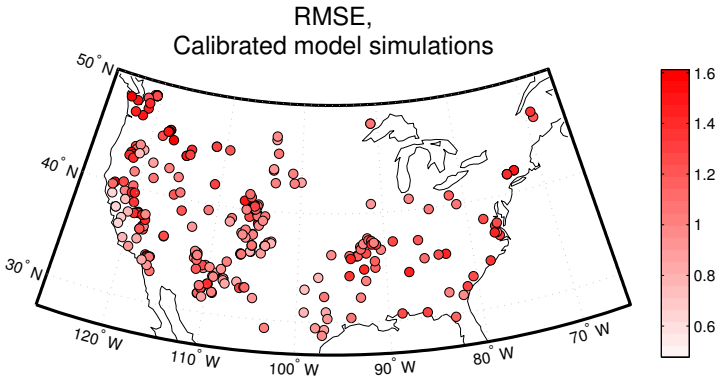

Figure 7: Root-mean-squared error of VS-Lite model residuals, compared to observed TRW series, across all simulation years, for simulations performed with parameters calibrated using the method described in this article.

Calibrated and uncalibrated simulated time series at two sites Here the calibrated and uncalibrated simulated ring-width time series are plotted with the observed ring-width time series for two sites. The first site, Geode State Park in Iowa, is an example where calibrating the model parameters results in a dramatic improvement in skill (correlation with observed series is $\rho = -0.30$ for uncalibrated simulation; $\rho = 0.63$ for the calibrated simulation). The second site, Andrew Johnson Woods in Ohio, was chosen as the site whose calibrated and uncalibrated correlations with the observed time series had the minimum mean distance from those correlations for all the other sites ($\rho = -0.13$ for uncalibrated and $\rho = 0.30$ for calibrated simulations). In that sense it represents a site with "typical" skill for both the uncalibrated and calibrated simulations.

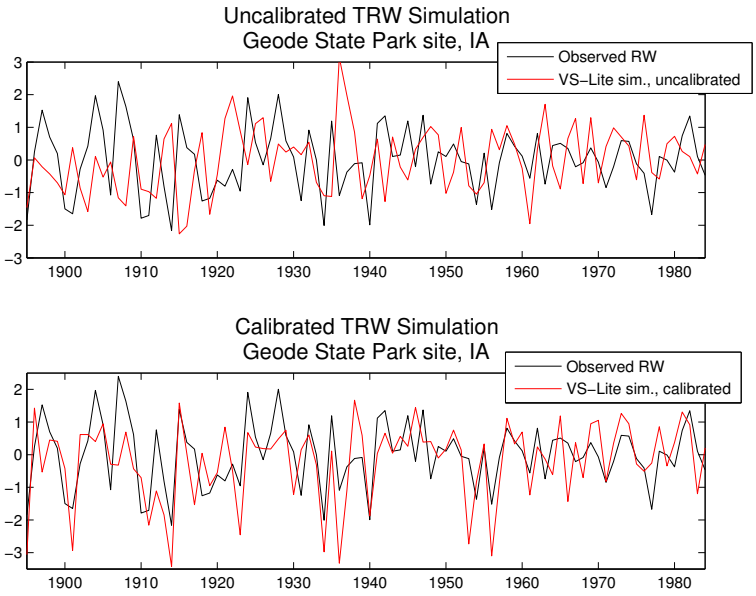

Figure 8: Time series of VS-Lite simulations of the White Oak chronology at the Geode State Park site in the southeastern corner of Iowa, using prior median parameters (top panel) and parameters calibrated by the method described in this paper (bottom panel). This site was chosen as an example where calibration makes a dramatic improvement in model simulation skill.

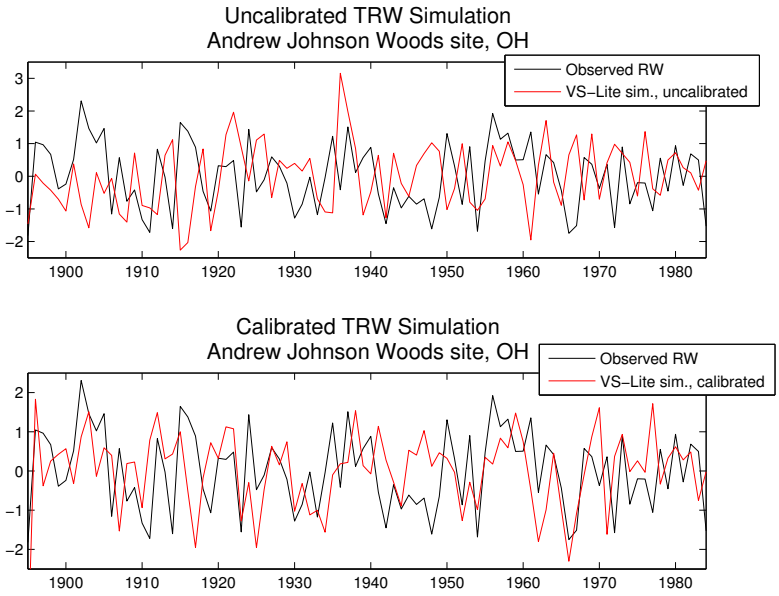

Figure 9: Time series of VS-Lite simulations of the White Oak chronology at the Andrew Johnson Woods site in Ohio, using prior median parameters (top panel) and parameters calibrated by the method described in this paper (bottom panel). This site was chosen as a more typical example of the improvement in simulation skill that results from calibrating the model parameters.